

## Enhanced superconducting properties of pre-doped B powder type MgB<sub>2</sub> strands

M.A. Susner, Y. Yang, M.D. Sumption, and E.W. Collings  
*CSMM, MSE, The Ohio State University, Columbus, OH 43210, USA*

M.A. Rindfleisch, M.J. Tomsic  
*Hyper Tech Research, Inc., 539 Industrial Mile Rd. Columbus, OH 43228, USA*

J.V. Marzik  
*Specialty Materials, Inc., 1449 Middlesex Street, Lowell, MA 01851, USA*

Conventional doping methods that directly add C or a C-bearing species to Mg+B powder have the disadvantage of adding C inhomogeneously, yielding either under-reacted regions or blocking phases. Pre-doped B powder provides a more homogeneous distribution of the C dopant in MgB<sub>2</sub>. Powders containing varying amounts of C were used to produce *in-situ* MgB<sub>2</sub> strands which showed high values of transport  $J_c$  ( $10^4$  A/cm<sup>2</sup> at 13.3T). Compared to SiC-added and malic acid-treated strands the pre-doped MgB<sub>2</sub> showed both higher values of  $B_{irr}$  and transport  $J_c$ , indicating that the pre-doping of B leads to more efficient C substitution into the B-sublattice.

Interest in MgB<sub>2</sub> as a superconducting material has been substantial, both because of practical considerations such as its relative ease of fabrication and mid-range  $T_c$  [1],[2], and more fundamental considerations which include its two-band nature [3]. Relevant to both of these categories, dopants which increase the irreversibility field,  $B_{irr}$ , and the upper critical field,  $B_{c2}$ , are subjects of particular interest, especially as the high values of  $B_{irr}$  and  $B_{c2}$  needed for applications are enabled by the two-band nature of the superconductor [3]. By far the most effective method of increasing the critical fields of MgB<sub>2</sub> is through addition of an element or compound that will lead to C-substitution into the B sub-lattice, producing disorder, thereby increasing  $B_{c2}$ , and hence the high field critical current density,  $J_c$  [4],[5]. This type of substitution also has the benefit of decreasing the critical field anisotropy [6]. The drop in  $T_c$  that is associated with C-doping-induced disorder is well known, but is a minor drawback when compared to the benefits of the resulting increases in  $B_{c2}$  and  $B_{irr}$ .

Two main categories of C-doping exist for the *in situ* MgB<sub>2</sub> superconductor. The first may be called *indirect addition*. Here a C-containing species is added that decomposes before or during the MgB<sub>2</sub> reaction to form free C that then substitutes into the B sublattice. However, this doping route, by its very definition, inevitably adds impurities. By far the most common example of such a C-containing species is SiC which during decomposition yields a by-product, Mg<sub>2</sub>Si, whose presence decreases the electrical connectivity between MgB<sub>2</sub> grains [7]. If we consider the relatively low reaction temperatures and times used in heat treating *in situ* wires, then we can assume that the diffusion of C into the B-sublattice is rather slow. As a result, the homogeneity of doping is determined by the distance between discrete dopant additions. We have already noted that C-doping by SiC results in a “smearing” of the superconducting heat capacity anomaly [8], which indicates that  $T_c$  is distributed over a wide range of temperatures indicating

that the level of doping in the superconducting strands is not uniform, resulting in chemical inhomogeneity.

The second category, *direct addition*, involves adding C to the Mg + B precursor powder mixture. Arguably the most successful example of this technique, at least in terms of resultant transport properties, is the malic-acid (MA) treatment, where MA is melted together with the precursor B at  $\sim 150^\circ\text{C}$  and subsequently pyrolyzed such that only C remains surrounding the B agglomerates. The homogeneity of the dopant distribution should therefore be more uniform than with the *indirect addition* method. However, because the reacted  $\text{MgB}_2$  grain size is, in the case of the *in-situ* method, strongly correlated with the operative length scales in the starting B powder (several micrometers down to less than 50 nm depending upon the type and provenance of the starting B powders), one now must consider the homogeneity of C-doping to be limited not by the size (spacing) of the dopant as is the case of SiC doping but by the size of the precursor B. Because the C is coating the precursor B, one would assume that, at least for the largest agglomerates, the C content on the outside of the final  $\text{MgB}_2$  grain will be higher than at the center. In addition, with the MA-treatment, it is seen that the C-coating of the B can serve to prevent Mg vapor from fully reaching some B, resulting in the presence of B-rich regions that remain even after aggressive heat treatments of  $700^\circ\text{C}$  and 8 hours [9]. In the doping of *ex-situ*  $\text{MgB}_2$  strands which will rely on C diffusion into the already formed (and typically larger grained)  $\text{MgB}_2$ , it is evident that the disadvantages of both *direct* and *indirect* C additions will be exaggerated.

Neither *direct* nor *indirect additions* will result in homogeneous doping unless the  $\text{MgB}_2$  is heat treated at very high temperatures for long times. Consequently to ensure a more

homogeneous distribution of C in MgB<sub>2</sub> at ordinary temperatures it is necessary to pre-dope the B powder.

For *in-situ* based MgB<sub>2</sub>, smaller B powder sizes lead to higher  $J_c$ s, presumably due to finer grain sizes in the final MgB<sub>2</sub> [10]. The most consistent method of producing pure B is through plasma spray synthesis in which BCl<sub>3</sub> gas is reduced by H<sub>2</sub> during the injection of both gasses into an RF plasma [11-13]. The resultant B is mostly amorphous with some nanocrystalline material. The plasma synthesis route also offers an opportunity to homogeneously dope with C through supplementing the gas stream with a hydrocarbon gas, e.g. CH<sub>4</sub>, thus providing nanocrystalline grains or amorphous powders which contain elemental C within the B powders themselves. Such C-containing B powders, as manufactured by Specialty Materials Inc (SMI), were obtained with a variety of C-doping levels enabling monofilamentary C-doped MgB<sub>2</sub> *in-situ* PIT strands to be manufactured.

Monofilamentary powder-in-tube (PIT) strands 0.83 mm in diameter with a Nb chemical barrier and a monel outer sheath (MgB<sub>2</sub>/Nb/monel) were manufactured by Hyper Tech Research, Inc. using a previously described process [14-16]. The starting powders consisted of Mg (99.9%, 20-25  $\mu$ m) and the SMI-C-doped B. Using a LECO CS600 inorganic combustion analyzer, the final B powders were found to have C contents of  $2.08 \pm 0.05$  wt% C,  $3.47 \pm 0.03$  wt% C,  $5.22 \pm 0.26$  wt% C, and  $7.15 \pm 0.11$  wt% C. Table I lists these values together with the doping levels, in mol%, of the final MgB<sub>2</sub> compound. Straight samples of the drawn wire  $\sim$ 20 cm in length were reacted under flowing Ar gas for 20 mins. at 700°C.

Four-point transport  $J_c$  measurements were made on short samples  $\sim$  3 cm long in fields of up to 14 T applied transversely to the strand. A voltage tap separation of 5 mm was used; the

$J_c$  criterion was 1  $\mu\text{V}/\text{cm}$ . SEM micrographs were taken on polished longitudinal cross-sections of the strands using back-scatter mode on a Phillips Sirion SEM with a FEG electron source.

For each SMI-C-doped sample resistivity measurements as function of temperature,  $R(T)$ , through the superconducting transition in transverse magnetic fields of from 0.01 to 14 T were made on samples 8 mm long using a Quantum Design Model-6000 physical property measurement system (PPMS). Samples were chemically stripped of the Ni-Cu outer sheath to avoid any effect on the measurement from this ferromagnetic material. After re-arranging the  $R(T,B)$  data, upper critical field and irreversibility field temperature dependencies,  $B_{c2}(T)$  and  $B_{irr}(T)$ , were then extracted based on the 10% and 90% resistive-transition points, Figure 1;  $\Delta T = B_{c2}(T) - B_{irr}(T)$ , was obtained as a function of field. As discussed in [17] there are several contributors to  $\Delta T$  such as: sample inhomogeneity or internal strain, thermally activated flux flow, and perhaps most importantly the Eisterer mechanism [18] which attributes the resistive transition to current percolation through a random mixture of grains whose anisotropic  $B_{c2}$ s are parameterized by  $\gamma = B_{c2}''/B_{c2}'$ : According to Eisterer

$$\Delta T = \left(1 - \sqrt{(\gamma^2 - 1)p_c^2 + 1}\right) B_0 / (\partial B_{c2} / \partial T) \quad (1)$$

in which  $\partial B_{c2} / \partial T$  is the critical field temperature dependence (Figure 1) and  $B_0$  denotes the external field. Based on this model and assuming 0.3 for the percolation threshold,  $p_c$ , as previously used in calculations of transport current percolation through porous  $\text{MgB}_2$  [19], we are able to show how critical field anisotropy depends of the level of C doping in our SMI-C samples, Figure 1(inset).

Figure 2 shows the 4.2 K transport  $J_c$ s as a function of magnetic field for various doping levels. Critical current densities of  $10^4 \text{ A}/\text{cm}^2$  were achieved at 6.4 T for the undoped  $\text{MgB}_2$ -00, 9.5 T for  $\text{MgB}_2$ -01, 10.9 T for  $\text{MgB}_2$ -02, 13.3 T for  $\text{MgB}_2$ -03, and 12.8 T for  $\text{MgB}_2$ -04. The

highest transport values were seen for MgB<sub>2</sub>-03, e.g. 10<sup>4</sup> A/cm<sup>2</sup> at 13.3 T. MgB<sub>2</sub>-04 exhibits lower  $J_{cs}$ , e.g. 10<sup>4</sup> A/cm<sup>2</sup> at 12.8 T, indicating that the C has exceeded its solubility limit [20] and is presumably collecting at the grain boundaries or in large clusters, thereby reducing connectivity.

Figure 3 presents the relationship between the analyzed C content of SMI-C-doped MgB<sub>2</sub> and the 4.2 K  $B_{irr}$  calculated using the 100 A/cm<sup>2</sup> criterion. A comparison to both SiC- added and MA treated samples is also presented. For these samples the C contents are based upon assuming complete disassociation of the SiC or LECO analysis of the MA-treated B powder. The pre-doped MgB<sub>2</sub> samples have the highest values of  $B_{irr}$  at every doping level. The MA-treated MgB<sub>2</sub> is relatively close to the pre-doped (SMI-C) line, suggesting that for this directly C-doped sample, substitution of C into the B sublattice is nearly complete. The microstructure typical of the MA-treatment, with areas of higher boride phases is also shown (Figure 3d).

Indirect C-addition via the 200 nm SiC-added MgB<sub>2</sub> sample leads to the greatest departure of  $B_{irr}$  from the SMI-C-doped line. This is a result of the relatively large size of the SiC particles and hence, for a given concentration, the relatively large distance between them which leads to a long C diffusion length. By contrast, the 15 nm SiC-added MgB<sub>2</sub> sample shows an increased value of  $B_{irr}$  for the same amount of SiC present, suggesting that the shorter distance between SiC particles resulting from the smaller particle size decreases the diffusion length, allowing more C to substitute into the B-sublattice thereby increasing  $B_{irr}$ . Also contributing to the departures of the SiC-doped  $B_{irr}$ s from the SMI-C-doped line is incomplete decomposition of the SiC particles as evidenced by the presence of unreacted SiC (Figure 3c). Again, it is seen that MgB<sub>2</sub>-04 does not follow the trend of the other pre-doped samples, with a visible plateau in  $B_{irr}$ .

at the expected doping level of 4.32 mol% C, once again suggesting that C has exceeded its solubility limit [20] in the B sublattice (Figure 3b).

In summary, Pre-doped B powders with various levels of C-doping were used to manufacture MgB<sub>2</sub> superconducting strands. These strands were found to have high 4.2 K transport  $J_c$  values, with sample MgB<sub>2</sub>-03 carrying  $10^4$  A/cm<sup>2</sup> at 13.3 T (154 kA/cm<sup>2</sup> at 6 T) and a  $B_{irr}$  of 23.5 T (as compared to 20.3 T and 16.1 T for 15 and 200 nm SiC additions with equivalent C contributions). An increase of the C content to 4.32%, marginally increasing  $B_{irr}$  to 24.4 T, but had a deleterious effect on  $J_c$ , then characterized by  $10^4$  A/cm<sup>2</sup> at 12.8 T. This phenomenon was attributed to dopant saturation where C formed clusters outside of the MgB<sub>2</sub> grains, serving to reduce electrical connectivity. The pre-doping mechanism was found to be a more efficient doping route than either the direct MA-treatment or indirect SiC addition, with higher critical fields reached for a given level of addition.

This work was supported by the United States Department of Energy, HEP grant DE-FG02-95ER40900.

- [1] J. Nagamatsu, N. Nakagawa, T. Muranaka Y. Zenitani, and J. Akimitsu, *Nature* **410**, 63-64 (2001).
- [2] P.C. Canfield, S.L. Bud'ko, and D.K. Finnemore, *Physica C* **385**, 1-7 (2003).
- [3] A. Gurevich, *Phys Rev. B* **67** 184515/1-13 (2003).
- [4] M.A. Susner, M.D. Sumption, M. Bhatia, X. Peng, M.J. Tomsic, M.A. Rindfleisch, and E.W. Collings, *Physica C* **456**(1-2), 180-187 (2007).
- [5] E.W. Collings, M.D. Sumption, M. Bhatia, M.A. Susner, and S.D. Bohnenstiehl, *Supercond. Sci. Tech.* **21**(10), 103001/1-14 (2008).
- [6] S. Oh, J.H. Kim, K. Cho, C. Lee, C.-J. Kim, S.X. Dou, M. Rindfleisch, M. Tomsic, and J.-H. Ahn, *J. Appl. Phys.* **106**, 063912/1-5 (2009).

- [7] A. Matsumoto, H. Kitaguchi, and H. Kumakra, *Supercond. Sci Tech.* **21**, 065007/1-6 (2008).
- [8] M.A. Susner, M. Bhatia, M.D. Sumption, and E.W. Collings, *J. Appl. Phys.* **105**(10) 103916/1-7 (2009).
- [9] M.A. Susner, “Macroscopic anisotropy and superconductivity in carbon-doped in-situ processed MgB<sub>2</sub> strands,” presented at EUCAS 2009, Dresden, Germany, 16 September 2009.
- [10] M.A.A. Mahmud, M.A. Susner, M.D. Sumption, M.A. Rindfleisch, M.J. Tomsic, J. Yue, and E.W. Collings, *IEEE Trans. Appl. Supercond.* **19**(3, Pt. 3), 2756-2759 (2009).
- [11] J.V. Marzik, R.J. Suplinskas, R.H.T. Wilke, P.C. Canfield, D.K. Finnemore, M.A. Rindfleisch, J. Margolies, and S.T. Hannahs, *Physica C* **423** 83-88 (2005).
- [12] J.V. Marzik, R.C. Lewis, M.E. Tillman, Y.Q. Wu, D.K. Finnemore, M. Rindfleisch, M. Tomsic, J. Yue, and W.J. Croft, *Mater. Res. Symp. Proc.* **1148**, PP12/01-6 (2008).
- [13] J.V. Marzik, R.C. Lewis, M.R. Nickles, D.K. Finnemore, J. Yue, M. Tomsic, M. Rindfleisch, and M.D. Sumption, *Adv. Cryo. Eng.* **56**, 295-301 (2010).
- [14] M.D. Sumption, M.A. Susner, M. Bhatia, M.A. Rindfleisch, M.J. Tomsic, K.J. McFadden, and E.W. Collings, *IEEE Trans. Appl. Supercond.* **17**(2, Pt. 3), 2838-2841 (2007).
- [15] M. Tomsic, M. Rindfleisch, J. Yue, K. McFadden, D. Doll, J. Phillips, M.D. Sumption, M. Bhatia, S. Bohnenstiehl, and E.W. Collings, *Physica C* **456**, 203-208 (2007).
- [16] M.D. Sumption, M. Bhatia, M. Rindfleisch, M. Tomsic, and E.W. Collings, *Appl. Phys. Lett.* **86**, 092507/1-3 (2005).
- [17] Z.X. Shi, M.A. Susner, M. Majoros, M.D. Sumption, X. peng, M. Rindfleisch, M.J. Tomsic, and E.W. Collings, *Supercond. Sci. Tech.* **23**, 045018/1-10 (2010).
- [18] M. Eisterer, M. Zehetmayer, and H.W. Weber, *Phys. Rev. Lett.* **90**(24), 247002/1-4 (2003).
- [19] A. Yamamoto, J.-I. Simoyama, Y. Katsura, S. Horii, K. Kishio, and H. Kumakura, *Supercond. Sci. Tech.* **20**, 658-666 (2007).
- [20] T. Takenobu, T. Ito, D.H. Chi, K. Prassides, and Y. Iwasa, *Phys. Rev. B* **64** 134513/1-3 (2001).



Table I. List of Sample Parameters

Sample Name	HTR Tracking #	SC fraction	wt% C in starting B powder	mol% C in final MgB <sub>2</sub>
MgB <sub>2</sub> -00	2134	0.252	0	0
MgB <sub>2</sub> -01	1990	0.115	2.08 ± 0.05	1.25 ± 0.03
MgB <sub>2</sub> -02	1650	0.152	3.47 ± 0.03	2.09 ± 0.02
MgB <sub>2</sub> -03	1991	0.131	5.22 ± 0.26	3.15 ± 0.16
MgB <sub>2</sub> -04	1952	0.183	7.15 ± 0.11	4.32 ± 0.07

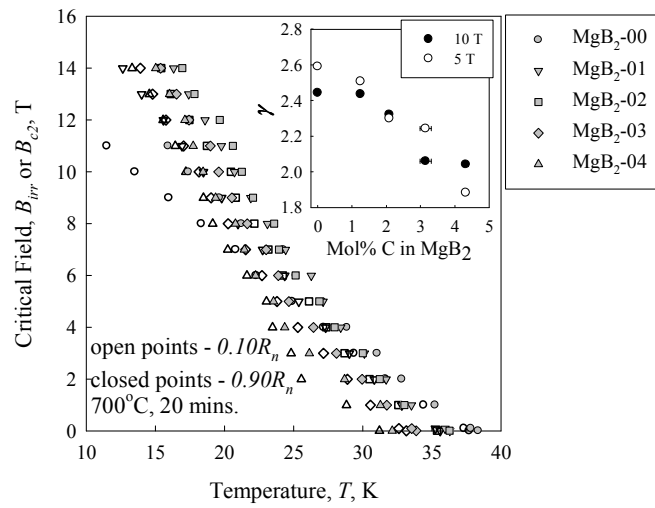


Figure 1. Critical fields,  $B_{irr}$  and  $B_{c2}$ , vs. temperature for various levels of C-doping. (Inset) Anisotropy ratio  $\gamma$  vs. mol%C at 5 T and 10 T.

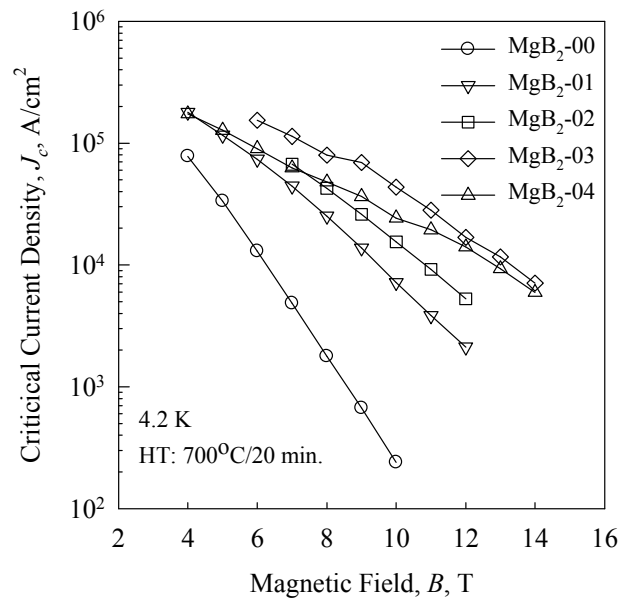


Figure 2. 4.2 K Transport  $J_c$  for increasingly C-doped MgB<sub>2</sub> strands.

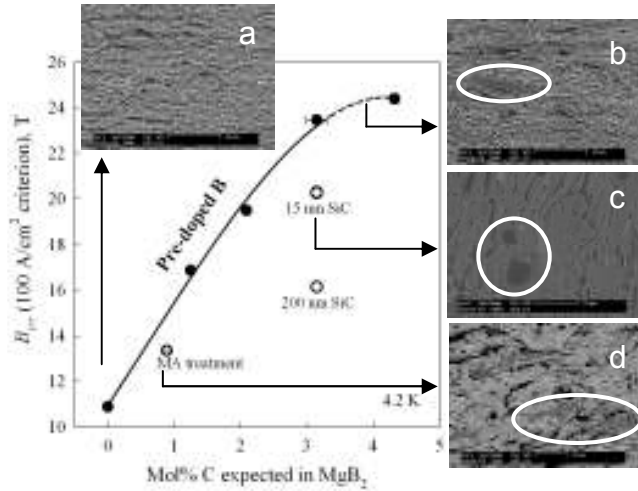


Figure 3.  $B_{irr}$  ( $100 \text{ A/cm}^2$  criterion) as function of expected C-doping for pre-doped  $\text{MgB}_2$ , SiC-added  $\text{MgB}_2$ , and MA-treated  $\text{MgB}_2$ . The microstructures for each method of C-doping are presented for comparison. (a) the undoped  $\text{MgB}_2$  shows a porous fibrous microstructure with no discernable inhomogeneities; (b) the heavily pre-doped  $\text{MgB}_2$  shows some areas of B- and C-rich impurity phases indicating C saturation; (c) the SiC-added  $\text{MgB}_2$  shows SiC agglomerations after HT; (d) the MA-treated  $\text{MgB}_2$  shows B-rich regions.